Drosophila contactin, a homolog of vertebrate contactin, is required for septate junction organization and paracellular barrier function

Catherine Faivre-Sarrailh[1,*,†], Swati Banerjee[2,*], Jingjun Li[2], Michael Hortsch[3], Monique Laval[1] and Manzoor A. Bhat[2,†]

[1]Neurobiologie des Interactions Cellulaires et Neurophysiopathologie, UMR 6184 CNRS, Institut Jean-Roche, Boulevard Pierre Dramard, 13916 Marseille Cedex 20, France
[2]Department of Cell and Molecular Physiology, Neuroscience Center and Curriculum in Neurobiology, University of North Carolina School of Medicine, Chapel Hill, NC 27599-7545, USA
[3]Department of Cell and Developmental Biology, University of Michigan, Medical School, Ann Arbor, MI 48109-0616, USA
*These authors contributed equally to this work
†Authors for correspondence (e-mail: sarrailh.c@jean-roche.univ-mrs.fr; manzoor_bhat@med.unc.edu)

Accepted 26 July 2004

Development 131, 4931-4942
Published by The Company of Biologists 2004
doi:10.1242/dev.01372

Summary

Septate junctions (SJs) in epithelial and neuronal cells play an important role in the formation and maintenance of charge and size selective barriers. They form the basis for the ensheathment of nerve fibers in *Drosophila* and for the attachment of myelin loops to axonal surface in vertebrates. The cell-adhesion molecules NRX IV/Caspr/Paranodin (NCP1), contactin and Neurofascin-155 (NF-155) are all present at the vertebrate axo-glial SJs. Mutational analyses have shown that vertebrate NCP1 and its *Drosophila* homolog, Neurexin IV (NRX IV) are required for the formation of SJs. In this study, we report the genetic, molecular and biochemical characterization of the *Drosophila* homolog of vertebrate contactin, CONT. Ultrastructural and dye-exclusion analyses of *Cont* mutant embryos show that CONT is required for organization of SJs and paracellular barrier function. We show that CONT, Neuroglian (NRG) (*Drosophila* homolog of NF-155) and NRX IV are interdependent for their SJ localization and these proteins form a tripartite complex. Hence, our data provide evidence that the organization of SJs is dependent on the interactions between these highly conserved cell-adhesion molecules.

Key words: Septate Junctions, F3/Contactin, Neurexin IV, Neuroglian, Axo-glial interactions

Introduction

The evolution of a unique set of intercellular junctions in multicellular organisms allows their regulation of the solute/solvent exchange and the preservation of the microenvironment of epithelial and excitable cells, thus preventing paracellular diffusion. Invertebrates and vertebrates evolved septate or tight junctions, respectively, to perform this function. In *Drosophila*, apicolateral SJs between epithelial cells act as functional analogs to the vertebrate tight junctions (Willott et al., 1993; Kirkpatrick and Peifer, 1995). They are characterized by regular arrays of electron-dense transverse structures or septa that span the intermembrane space and form a physical barrier to diffusion (Auld et al., 1995; Baumgartner et al., 1996). Besides serving as a paracellular barrier to diffusion, SJs play additional roles in the maintenance of epithelial polarity and cell adhesion in *Drosophila* (Woods et al., 1996) (S.B. and M.B., unpublished). In *Drosophila* nervous system, SJs are formed by the perineurial glial cells that ensheath the nerve fibers (Bellen et al., 1998). In vertebrates, SJs are encountered at the axo-glial interface in the paranodal region of myelinated nerve fibers, acting as ionic barriers and molecular fences to maintain distinct molecular domains at the nodes of Ranvier (Bhat et al., 2001; Boyle et al., 2001; Rios et al., 2003) (for a review, see Bhat, 2003).

Several molecular components of the vertebrate axo-glial SJs have been identified, which include NCP1, contactin and NF-155 as the major cell-adhesion molecules (CAM) (Girault and Peles, 2002). F3/F11/contactin is a GPI-anchored CAM that contains immunoglobulin domains linked to fibronectin type III (FNIII) repeats (Gennarini et al., 1989; Brümmendorf and Rathjen, 1996). In vertebrates, contactin is predominantly expressed by neurons and has been implicated in the control of axonal growth and fasciculation through heterophilic interactions with multiple ligands (Berglund et al., 1999; Falk et al., 2002), including the L1-type molecules, L1-CAM, NrCAM and neurofascin (Brümmendorf and Rathjen, 1996).

A major role of contactin in myelinated fibers is to organize axonal subdomains at the nodes of Ranvier. The nodal region is highly enriched in voltage-gated Na^+ channels, thereby allowing the rapid saltatory conduction of the action potential. At either end of the node, in the paranodal region, a series of septate-like junctions anchors the myelin terminal loops to the axolemma. Contactin is an essential axonal component of the paranodal SJs, where it forms a cis-complex with NCP1 (Menegoz et al., 1997; Peles et al., 1997). Deficiency in either

NCP1 or contactin results in a loss of SJs and an aberrant organization of the paranodal region, which causes a severe reduction in nerve conduction velocity (Bhat et al., 2001; Boyle et al., 2001). The glial ligand NF-155 was shown to form a ternary complex with NCP1 and contactin at the axon-glial interface of the paranodes (Charles et al., 2002).

Nerve ensheathment in *Drosophila* and myelination in vertebrates share important common features, including process extension around axons and formation of SJs, which isolate the nerve fibers from the extracellular fluid (Bellen et al., 1998; Einheber and Salzer, 2000). NRX IV (NRX – FlyBase), the fly homolog of NCP1, plays a crucial role in the formation of SJs in perineurial glial cells in the peripheral nervous system (PNS) and is required for the integrity of the blood-nerve barrier and the proper conduction of nerve impulses (Baumgartner et al., 1996). NF-155 belongs to the L1-type family which in *Drosophila* is encoded by a single gene, *nrg* (Bieber et al., 1989; Hortsch, 2000). Recent studies have suggested the role of NRG along with other components such as gliotactin and Na^+K^+ATPase in the formation of SJs (Genova and Fehon, 2003; Schulte et al., 2003). In order to better understand the formation and function of SJs and to investigate the parallels that exist between *Drosophila* and vertebrate SJs, additional components of SJs need to be identified. The physiological interaction between vertebrate NCP1 and contactin suggested that a similar molecular complex might exist at the invertebrate SJs. In the present study, we report the characterization of the *Drosophila* homolog of vertebrate contactin referred here as *Drosophila* Contactin (CONT), which co-localizes with NRX IV and NRG at epithelial SJs and in perineurial glial cells of the PNS. Our biochemical data indicate that they form a tripartite complex. Ultrastructural and dye-exclusion analyses demonstrate that CONT plays an important role in the organization of SJs and maintenance of a functional paracellular barrier. Our studies thus provide evidence that the paranodal SJs of myelinated fibers in vertebrates may share their evolutionary origin with invertebrate SJs, thus making them amenable to comparable genetic and molecular analysis.

Materials and methods

Drosophila stocks

The P element strain KG9756 was obtained from Hugo Bellen. *nrx IV^{4304}* allele has been described previously (Baumgartner et al., 1996). *nrg^1* flies were obtained from L. Garcia-Alonso. The deficiency stock *Df(3R)XM3* was obtained from the Bloomington Stock Center.

Cloning of *cont*

Total RNA from II and III instar larvae was extracted using TRIzol (Invitrogen) and cDNA synthesis was carried out with the SuperScript system (Invitrogen) according to the manufacturer's instructions. The full-length cDNA of *cont* was cloned in two steps using PCR amplification with Expand High Fidelity PCR system (Roche). First, the 5′ half of *cont* cDNA (2163 bp) was amplified starting at position 580 of the FlyBase transcript sequence, using the 5′GCCTTTAGTCT-GCTGCGAGA3′ sense primer and the 5′TCATAGACAGCACTCG-GAGCT3′ antisense primer. This fragment was inserted into the *Not*I-*Xba*I cloning sites of *pP{CaSpeR-hs}* transformation vector (Thummel et al., 1988). Second, the 3′ half of the cDNA sequence (2359 bp) was amplified using the 5′CCGGAAGACACTTATGAAG-AGC3′ sense primer and the 5′CAAGAGAAGCACGGATGGAAT3′ antisense primer. Subsequently, this fragment was inserted into *Xba*I-digested *pP{CaSpeR-hs}* vector DNA, which contained the 5′ half of the *cont* cDNA. The complete sequence of the PCR amplified regions was established by Genome Express (France). The full-length cDNAs of *cont* and *nrx IV* were subcloned into pCDNA3 (Invitrogen) for mammalian cell expression experiments.

Generation of CONT antibodies

A recombinant protein was generated using the *pQE30* vector (Qiagen), which carried a his-tag fused to Ig5-6 domains and the hinge region of CONT (corresponding to amino acid residues 772-1138). After induction, the his-CONT fusion protein was purified under denaturing conditions by affinity chromatography on Ni-agarose beads and used for the immunization of rats. For the production of polyclonal antisera in guinea pigs, the cDNA coding for 172 amino acids of CONT (residues 24-195) was fused to a his-tag in *pET28a(+)* (Novagen) and expressed in *E. coli* BL21DE3. The recombinant protein was purified from a preparative SDS-PAGE gel and used for the immunization of guinea pigs.

Generation of *cont* mutants and transgenic flies

The P element KG9756 was mobilized to generate imprecise excisions as previously described (Bhat et al., 1999). To generate a genomic rescue construct, a cosmid library was obtained from John Tamkun (Tamkun et al., 1992). A 7 kb *Spe*I-*Spe*I fragment which contained the entire *cont* gene was cloned in *pP{CaSpeR-4}*, and for heat-shock induced *cont* expression, *cont* cDNA was cloned into *pP{CaSpeR-hs}*. The recombinant plasmids were used for germline transformation to obtain transgenic flies. For heat-shock experiment, 4- to 10-hour old embryos from the parental genotype *hs-cont/hs-cont; cont^{ex956}/TM3,Sb,dfd-lacZ* were heat-shocked at 37°C for 60 minutes followed by recovery for 7 hours at room temperature, and processed for immunohistochemical analysis.

Immunohistochemistry

Wild-type and mutant embryos from *cont^{ex956}*, *nrx IV^{4304}* and *nrg^1* were collected and aged for 12-18 hours at 25°C. Embryos were processed for immunostaining as previously described (Bhat et al., 1999). The following primary antibodies were used: guinea pig anti-CONT (1:2000) (this study), rat anti-CONT (1:500) (this study) and rabbit anti-NRX IV (1:2000) (Baumgartner et al., 1996). Monoclonal anti-NRG antibodies 1B7 and 3C1 have been described previously (Bieber et al., 1989; Hortsch et al., 1995). Secondary antibodies used for immunofluorescence were obtained from Jackson ImmunoResearch. Confocal images were captured on a BioRad Radiance 2000 Confocal Microscope and the image files were processed using Photoshop Software.

Electron microscopy and dye exclusion assay

cont^{ex956} and *nrg^1* mutant embryos were identified against a GFP-expressing balancer chromosome. Mutant and wild-type embryos aged 19-21 hours at 20°C were hand-dechorionated, perforated with a tungsten needle and fixed with 2.5% glutaraldehyde in 50 mM cacodylate buffer (pH 7.2) for 2 hours, post-fixed in 1% osmium tetraoxide for 1 hour, en bloc stained with uranyl acetate, dehydrated and embedded in Spurr. Ultrathin sections were contrasted with uranyl acetate and examined on a Philips CM10 electron microscope. For the dye exclusion assay, rhodamine-labeled 10-kDa dextran (Molecular Probes) was injected into the body cavity of stage 16 embryos as described by Lamb et al. (Lamb et al., 1998).

Immunoprecipitation and western blot analysis

Embryos (18 hours) were homogenized in 10 mM Tris buffer (pH 7.5), which contained 0.32 M sucrose and protease inhibitors (1 mM PMSF, 5 μg/ml α-2-macroglobulin, 1 μg/ml leupeptin and 5 μg/ml pepstatin). The homogenate was centrifuged for 10 minutes at 1500 ***g***. The supernatant was centrifuged at 100,000 ***g*** for 1 hour and the microsomal fraction was solubilized for 30 minutes in 50 mM Tris

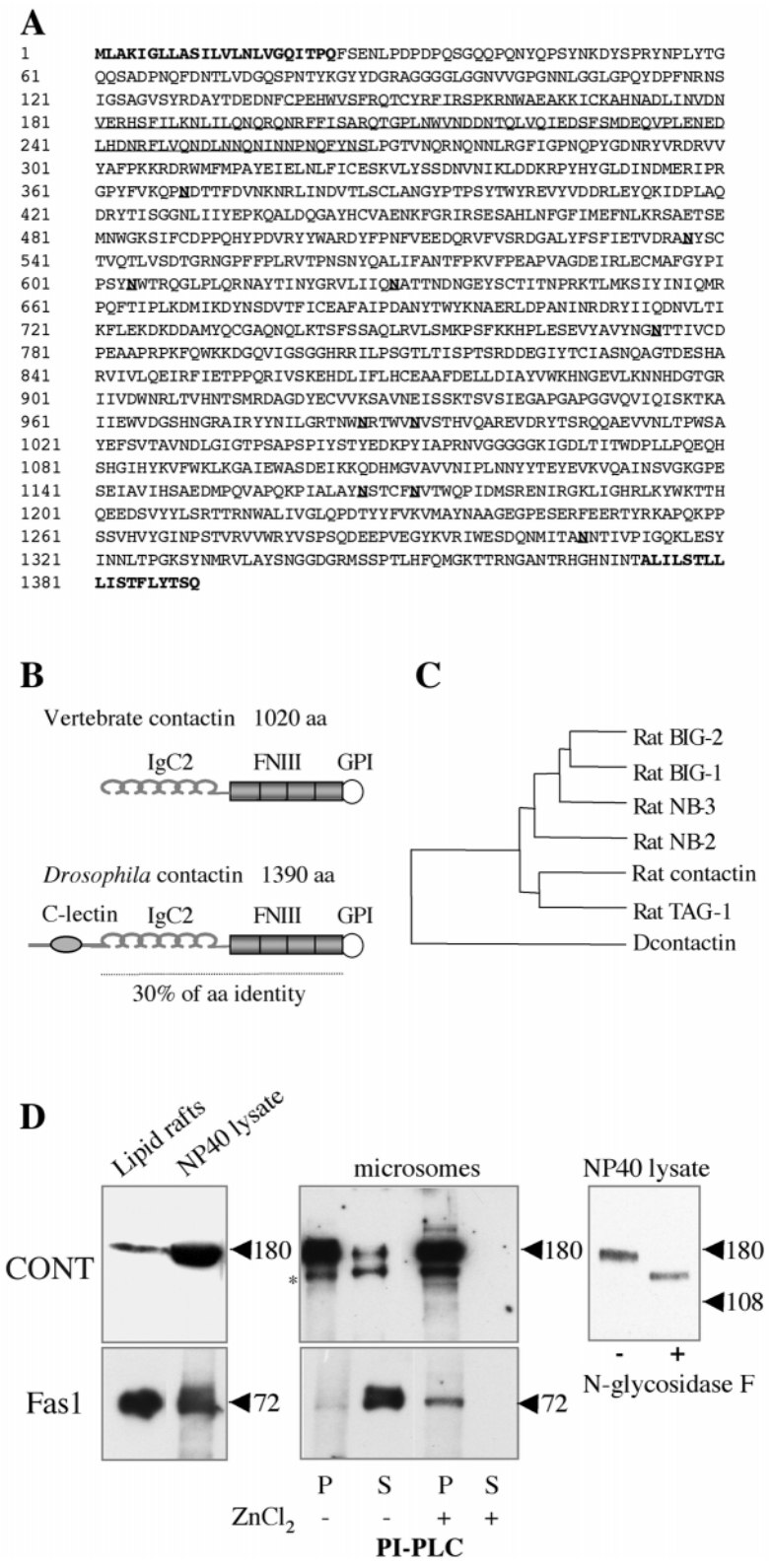

Fig. 1. CONT represents the single *Drosophila* homolog of the vertebrate contactin family. CONT is encoded by the transcriptional unit CG1084 (FlyBase), which was predicted from the *Drosophila* genome sequence. (A) The translation of *cont* cDNA reveals an ORF of 1390 amino acids. The signal peptide and the GPI anchor signal are indicated in bold. The C-lectin domain is underlined. The predicted N-glycosylation sites are marked in bold and are underlined. These sequence data are available from GenBank under Accession Number AY229991. (B) The modular protein domain structure for the CONT protein is shown in comparison with vertebrate contactin. Except for the N-terminal C-lectin domain in CONT, both proteins display a similar domain organization. (C) The phylogenetic tree obtained after aligning the protein sequences encoding rat contactin, TAG-1, NB-2, NB-3, BIG-1 and BIG-2 with the *Drosophila* CONT sequence. For this phylogenetic tree analysis, the CONT C-lectin domain was not considered. (D) Immunoblots of lipid rafts and microsomes that were prepared from 18-hour-old embryos. (Left panel) A single protein band with an apparent molecular weight of ~180 kDa can be detected in both fractions when probed with the guinea-pig anti-CONT antiserum, which is directed against the N-terminal C-lectin domain. As a control, Fas1 is highly concentrated in the lipid raft fraction. (Middle panel) The microsomes were incubated with PI-PLC in the presence or absence of $ZnCl_2$ followed by high-speed centrifugation. Solubilized pellet (5 μl) (P) and 25 μl of supernatant (S) were analyzed. As shown in the middle panel, a significant proportion of CONT was released in the supernatant after PI-PLC treatment. This release of CONT from the microsomal pellet was completely inhibited by the presence of $ZnCl_2$. The asterisk shows a degradation band that resulted from incubation at 37°C. As a control, the major fraction of Fas1 was cleaved by PI-PLC and recovered in the supernatant, this release was also inhibited by the presence of $ZnCl_2$. (Right panel) N-glycosidase-F treatment of the microsomal NP-40 extracts reduces the size of CONT to ~155 kDa, close to the size predicted from the cDNA sequence (158 kDa).

buffer (pH 7.5), 1% NP-40. After preclearing for 2 hours at 4°C with protein A-Sepharose, the supernatant was immunoprecipitated overnight at 4°C with protein A Sepharose, which had been coated with either anti-NRX IV antibody (3 μl), with rabbit-anti-mouse immunoglobulins and 1B7 or 3C1 ascites fluid (5 μl) or with guinea pig anti-CONT (3 μl). For the rat anti-CONT immune serum (5 μl), anti-rat agarose beads were used instead. The beads were washed twice with 50 mM Tris buffer (pH 7.5), 150 mM NaCl, 1% NP-40, twice with 50 mM Tris buffer, 150 mM NaCl, and twice with 50 mM Tris buffer. Immunoprecipitates were analyzed by immunoblotting using anti-CONT, anti-NRX IV or anti-NRG (3C1) antibodies in a standard western blotting procedure. Control experiments with

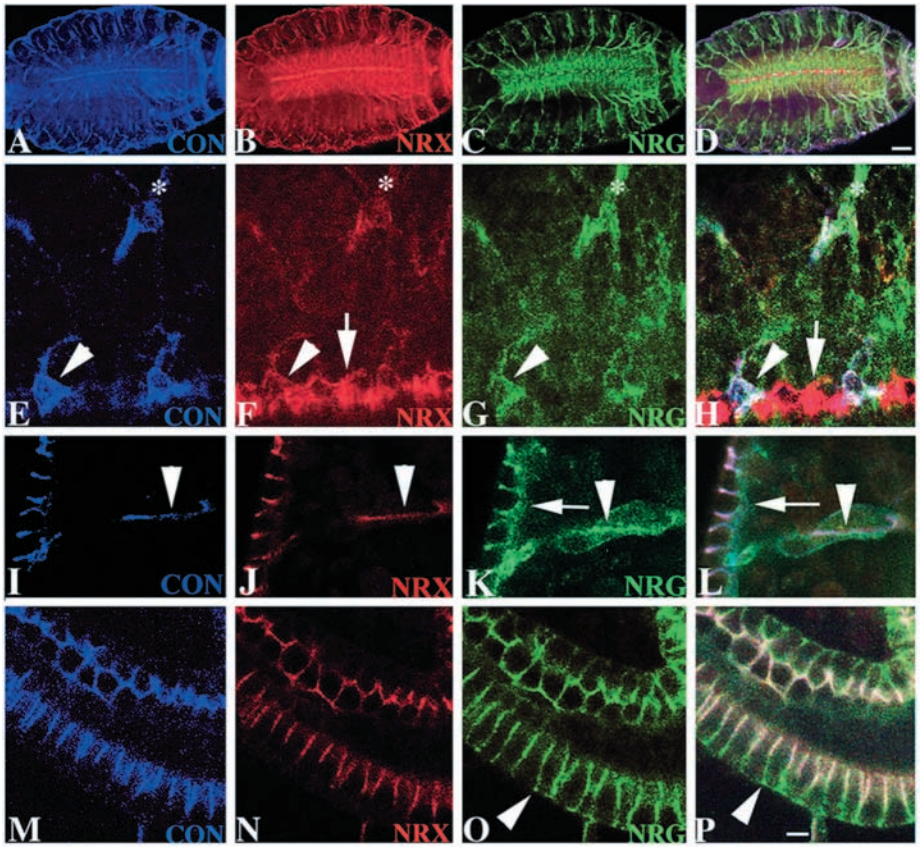

Fig. 2. CONT is expressed in ectodermal epithelia and glial cells of the PNS in *Drosophila* embryos. (A-D) A confocal section of a whole-mount stage 16 wild-type embryo triple stained with anti-CONT (A, blue), anti-NRX IV (B, red) and anti-NRG (C, green). CONT is expressed in all the ectodermally derived epithelial cells, including epidermis, salivary glands, trachea, hindgut and peripheral glial cells. The focus is on the midline of the CNS and the exiting axon tracts and parts of the epidermis. The merged image of the three panels is shown in D. Scale bar: 50 μm for A-D. (E-H) Part of the CNS midline and peripheral glial cells at a higher magnification shows that CONT (E, blue) and NRG (G, green) are not expressed in midline glial cells where NRX IV is strongly expressed (F, red, see arrow pointing to the midline glial cells). The roots of the glial cells, which ensheath axonal commissures in the CNS, express all three proteins (E-H, arrowheads). In the peripheral nerves, the expression pattern of all three proteins overlap (asterisks). (I-L) A region of the epidermal epithelial cells at a higher magnification demonstrates that CONT (I, blue), NRX IV (J, red) and NRG (green) are co-expressed at SJs (L, merged color white). NRG expression extends more basolaterally (arrow in K and L), whereas CONT and NRX IV are restricted to SJ domains. The arrowheads in I-L indicate overlapping expression along the peripheral nerve. (M-P) Part of the hindgut at a higher magnification also shows that CONT (M, blue), NRX IV (N, red) and NRG (O, green) are concentrated at SJs, but that NRG extends more basolaterally (arrowheads in O and P). Scale bar: 16 μm for E-P.

uncoated protein A-Sepharose or with agarose beads coated with anti-CONT pre-immune serum, yielded negative results.

The lipid rafts from embryos (18 hours) were prepared as low density Triton X-100-insoluble complexes as described previously (Faivre-Sarrailh et al., 2000). Phosphatidylinositol-phospholipase C (PI-PLC) treatment was carried out as described by Gennarini et al. (Gennarini et al., 1989). Briefly, 100 μl aliquotes of microsomes from 18-hour-old embryos were first incubated for 2 hours at 37°C to eliminate spontaneously released proteins and then were treated threefold with 0.2 unit PI-PLC (GlycoSystems, Oxford) for 40 minutes. After ultracentrifugation at 100,000 ***g***, pellets were resuspended in 100 μl and supernatants were analyzed by immunoblotting with anti-Fasciclin 1 (Fas1) (Hortsch and Goodman, 1990) and anti-CONT antibodies. The N-glycosylation pattern of CONT was examined using N-glycosidase-F (Roche). The NP-40 extracts and lipid raft fractions were incubated for 3 hours in 0.2% SDS and 1% β-mercaptoethanol with N-glycosidase-F (20 units/ml).

Transient transfection of N2a cells

N2a cells were grown in DMEM (Invitrogen) containing 10% FCS, as well as penicillin (50 U/ml) and streptomycin (50 μg/ml). Transient transfections with *pCDNA3-nrx IV* or *pCDNA3-cont* were carried out using Lipofectamin Plus (Invitrogen). After 48 hours, cells were fixed with 4% PFA in PBS, permeabilized with 0.1% Triton X-100 in PBS and processed for immunostaining. Double-immunostaining was performed with anti-CONT and anti-BiP mab (StressGen, Tebu) as an ER marker. In some experiments, living cells were immunostained for CONT and then fixed, permeabilized and processed for immunostaining for NRX IV.

Results

Structural comparison between CONT and its mammalian homologs

The vertebrate contactin subfamily of GPI-anchored Ig-CAMs comprises TAG-1/axonin-1, and several other related proteins, BIG-1, BIG-2, NB-2/FAR-2 and NB-3 (Furley et al., 1990; Yoshihara et al., 1995; Ogawa et al., 1996; Plagge et al., 2001). A Blast search of the *Drosophila* genome using the human contactin sequence identified a single *Drosophila* gene, CG1084 (FlyBase), with high sequence homology to contactin family members, which was named *cont*. We amplified the *cont* cDNA by RT-PCR from larval mRNA and sequenced three independent clones. This revealed an open reading frame of 1390 amino acids residues (Fig. 1A). Northern blot hybridization using a *cont* cDNA probe revealed a single band of ~4.3-4.5 kb (data not shown). Further RT-PCR analysis gave no indication that *cont* undergoes alternative splicing. The primary protein structure of CONT encompasses a N-terminal signal peptide, a C-lectin domain, six Ig domains, four FNIII repeats and a consensus sequence for GPI-anchor addition (Fig. 1A). Except for the presence of the C-lectin domain at the N terminus, the modular domain organization of CONT is similar to vertebrate contactin (Fig. 1B). A phylogenetic analysis indicates that CONT is the *Drosophila* representative of the vertebrate contactin family (Fig. 1C).

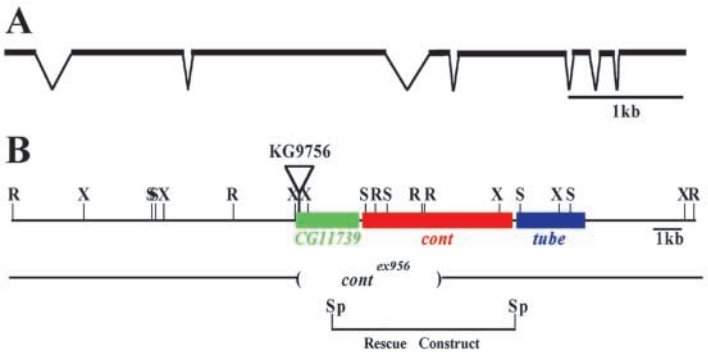

Fig. 3. Genomic structure of the *cont* locus and generation of *cont* mutants. (A) Based on the FlyBase genomic sequence information, the *cont* gene spans ~5.7 kb. Comparison of the genomic (FlyBase) and cDNA (Accession Number AY229991) sequences revealed that the *cont* locus is composed of eight exons (black bars) with intronic sequences ranging from 53 to a maximum of 350 nucleotides. (B) Genomic map of ~17 kb region that includes *CG11739*, *cont* and *tube*. The P element (KG9756) is inserted in the first intron of *CG11739*. *cont* is within ~100 bp downstream of *CG11739*, followed by *tube* within 300 bp. These loci are unusually close to each other. A chromosomal deficiency *Df(3R)XM3* that uncovers this region deletes *cont* and the neighboring loci. One of the imprecise excisions from KG9756 mobilization removes ~5 kb of the genomic region resulting in the loss of *CG11739* and *cont*. A 7 kb *Spe*I (Sp) genomic construct rescues the lethality of $cont^{ex956}$ to adulthood.

CONT is a GPI-anchored membrane glycoprotein

To determine the relative molecular mass of the CONT protein, we generated polyclonal antibodies in rat and guinea pig against two his-tagged recombinant proteins, which contained Ig domains 5 and 6 with the hinge region or the N-terminal region containing the C-lectin domain, respectively. Embryonic extracts from 18-hour-old *Drosophila* embryos were prepared to obtain microsomal fractions, which were solubilized in NP-40, followed by western blot analysis. Both antisera detected a major single band of ~180 kDa compared with a predicted size of 158 kDa (Fig. 1D). Rat and guinea pig preimmune sera consistently did not detect this 180 kDa protein band (not shown). As CONT sequence contains 10 putative N-glycosylation sites (Fig. 1A), the larger than expected apparent size of CONT may be the result of an extensive glycosylation. To test this hypothesis, microsomal fractions were treated with N-glycosidase F. As shown in Fig. 1D, deglycosylation of the 180 kDa band results in a ~155 kDa band, corresponding to CONT protein core. CONT, which contains a GPI-anchor motif is recovered in the detergent insoluble lipid raft fraction like the GPI-anchored cell adhesion molecule Fas1 (Hortsch and Goodman, 1990) (Fig. 1D). In addition, CONT can be released from embryonic microsomal fraction by PI-PLC treatment. Only a fraction of CONT was sensitive to PI-PLC cleavage, whereas almost all Fas1 from the same microsomal fraction was cleaved by PI-PLC (Fig. 1D). These data show that CONT is a GPI-anchored membrane associated glycoprotein.

CONT is expressed in epithelial cells and glial cells of peripheral nerves

To determine the expression pattern of the CONT protein, 0- to 16-hour-old embryos were immunostained with anti-CONT antibodies. Both guinea pig and rat anti-CONT antibodies revealed that CONT is expressed in ectodermally derived epithelial cells from stage 12. All these tissues, such as epidermis, hindgut, foregut, salivary glands and trachea, have been shown to contain pleated SJs (Tepass and Hartenstein, 1994; Baumgartner et al., 1996). To establish the subcellular localization of CONT more precisely and to compare its distribution with that of NRX IV, a known SJ specific protein, and NRG, a homolog of the vertebrate axo-glial SJ component NF-155, co-immunolocalization studies of wild-type embryos were carried out using guinea pig anti-CONT (Fig. 2A, blue), anti-NRX IV (Fig. 2B, red) and anti-NRG (Fig. 2C, green). This triple labeling showed that CONT expression overlaps with that of NRX IV and NRG in most epithelial tissues in which these molecules are co-expressed (Fig. 2D, merge). Furthermore, the onset of CONT and NRX IV expression detected by immunostaining is identical and, like NRX IV, CONT does not have any maternal contribution (data not shown). NRX IV is expressed in perineurial glial cells, which insulate peripheral nerves, and in the midline glial cells that ensheath anterior and posterior commissures. CONT colocalizes with NRX IV in perineurial glial cells of peripheral nerves (Fig. 2E,F, asterisks), whereas it shows a distribution clearly distinct from NRX IV in the midline glial cells (Fig. 2F,H, arrows). As NRG is strongly expressed in the peripheral nerves (Fig. 2G, asterisk), regions of overlap between the three markers are shown in the merged image (Fig. 2H, asterisk). In the midline, some of the glial cells express CONT, NRX IV and NRG, as indicated by intense white color (Fig. 2H, arrowhead pointing on the midline).

The expression pattern of CONT is similar to those of other septate junction markers such as coracle, which is expressed by ectodermally derived epithelial cells and along peripheral nerves although it is not present in midline glial cells (Fehon et al., 1994; Baumgartner et al., 1996; Ward et al., 1998). Unlike NRX IV, CONT is not expressed in midline glial cells, indicating that NRX IV may have additional partners in the midline glial cells.

CONT is a component of epithelial SJs

In *Drosophila*, epithelial tissues of the epidermis and hindgut contain SJs along the apicolateral domain below the zonula adherens or adherens junctions. To determine whether CONT precisely localizes to SJs in the epidermis and the hindgut, confocal microscopy images of these tissues, which focus on the epithelial cells, were captured at high magnification. As shown in Fig. 2I-L, CONT, NRX IV and NRG display almost complete colocalization at the SJs of epidermal cells (as indicated by the merged white color in Fig. 2L). Although, NRG is clearly enriched at SJs, it exhibits a broader distribution and is also expressed along the basolateral membrane (Fig. 2K,L, white arrows). In addition, all three proteins colocalize along the peripheral nerves where SJs

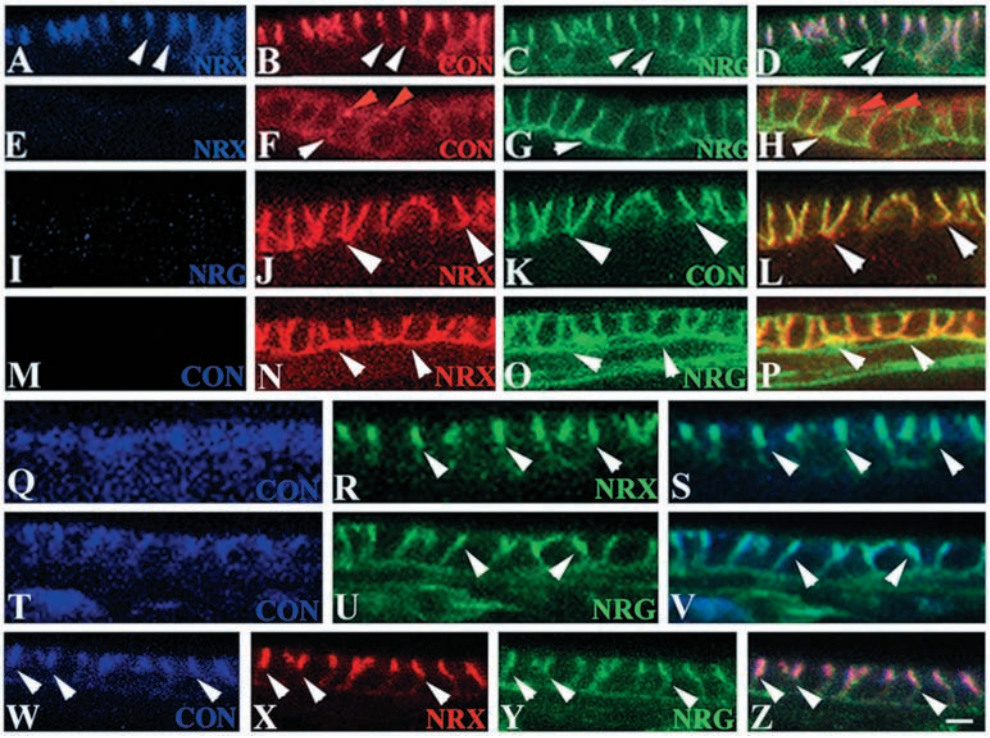

Fig. 4. NRX IV, NRG and CONT are interdependent for their localization at the SJs. (A-D) This region of the wild-type epidermis at stage 16 shows the SJ localization of NRX IV (A, blue), CONT (B, red) and NRG (C, green), and the merged image (D). (E-H) Epidermis from a *nrx IV*^{4304}*/nrx IV*^{4304} embryo at stage 16 with a loss of NRX IV protein (E, blue), a diffuse localization of CONT around the cell cortex (F, red) and a uniform basolateral localization of NRG (G, green). White arrowheads indicate the basolateral distribution of NRG (compare G with C). CONT is also seen in intracellular vesicles, as indicated by red arrowheads in F and H. (I-L) This part of the epidermis from a *nrg*^{1}*/Y* embryo at stage 16 shows the loss of NRG staining (I, blue). White arrowheads indicate the basolateral distribution of both NRX IV (J, red) and CONT (K, green). Compare the merged image L with D. (M-P) Part of the epidermal epithelial layer from homozygous *cont*^{ex956} mutant embryo at stage 16, showing total loss of CONT (M, blue) and mislocalization of NRX IV (N, red) and NRG (O, green) along the basolateral area, as indicated with arrowheads (N-P). Merged image in P. (Q-V) Epidermis from *hs-cont/hs-cont;cont*^{ex956}*/cont*^{ex956} homozygous embryos at stage 16 heat-shocked to induce the expression of CONT (Q and T, blue), show that NRX IV (R, green) or NRG (U, green) localization at SJs has been restored (compare arrowheads in R with N or in U with O). Merged images are shown in S and V. (W-Z) Epidermis from *cont*^{ex956}*/cont*^{ex956} embryo rescued by *Spe*I genomic fragment at stage 16 shows normal expression and localization of CONT (W), and restoration of NRX IV (X) and NRG (Y) to SJs. A merged image of these proteins is shown in Z. Arrowheads indicate localization of these proteins at SJs. Scale bar: 16 μm.

have been identified (Fig. 2I-L, arrowheads). Similarly, we determined the distribution of CONT in hindgut epithelial cells, which are more columnar than epidermal epithelial cells. As shown in Fig. 2M-P, CONT, NRX IV and NRG colocalize at SJs, and here NRG also shows an additional basolateral localization (Fig. 2O,P, arrowheads). Thus, the immunohistochemical analysis shows that CONT, NRX IV and NRG are co-expressed at SJs.

Genomic structure of *cont* and generation of *cont* mutants

To determine the in vivo function of CONT, we initiated a genetic analysis of the *cont* locus. Based on the genomic sequence information, the *cont* gene maps to 82A6-B1 and spans ~5.7 kb with eight exons (Fig. 3A). A deficiency chromosome *Df(3R)XM3,ru*^{1}*th*^{1}*st*^{1}*kni*$^{ri-1}$*cu*^{1}*p*^{p}*e*^{1}*/TM3,Sb*^{1} *(082A03-06;082B)* that uncovered *cont* locus, was obtained from the *Drosophila* Stock Center and examined by Southern blot analysis to determine whether the *cont* locus was deleted and also by immunohistochemical analysis using anti-CONT antibodies to determine whether the deficiency homozygous embryos were lacking the CONT protein. Southern blot analysis using a region of the *cont* cDNA as a probe showed half-signal intensity in *Df(3R)XM3* when compared with wild-type signals confirming the deletion of the *cont* gene in *Df(3R)XM3* chromosome (data not shown). Immunohistochemistry using anti-CONT antibodies further established that *Df(3R)XM3/Df(3R)XM3* homozygous embryos did not produce any CONT protein.

As there are no chemically or P element-induced mutations in *cont* gene, loss-of-function mutants had to be generated. To initiate the mutational analysis in the *cont* gene, we identified a viable P element KG9756 (*y*^{1}*; ry*^{506} *P{y*$^{+mDint2}$ *w*$^{+BR.E.BR}$*= SUPor-P}*) that had inserted in the neighboring gene, *CG11739* (Fig. 3B). This gene encodes a mitochondrial tricarboxylate-carrier activity and is located in the 5′ end of the *cont* locus. The P-element insertion site is ~2.5 kb from the predicted 5′ end of *cont* (Fig. 3B) and ~3.2 kb from its ATG start codon. The transcription start site (predicted by FlyBase) of the *cont* locus is just 90 bp from the 3′ end of *CG11739*. Standard P element mobilization procedures were followed (Bhat et al., 1999) to obtain imprecise excisions. We screened approximately 3000 individual chromosomes and obtained 13 lethal lines over *Df(3R)XM3* deficiency, 11 of which showed complete loss of CONT. By carrying out Southern blot analysis, we narrowed down the breakpoints in one of the excision lines (*cont*^{ex956}) that started from the P insertion site and deleted ~5 kb towards the *cont* locus. This excision causes embryonic lethality. To rescue the lethality of the *cont*^{ex956} excision, we generated transgenic lines using a 7 kb *Spe*I-*Spe*I genomic fragment, which breaks in the middle of *CG11739* (deleting its promoter region and the first 144 amino acids out of a total of 321 amino acids) and has intact *cont* locus (Fig. 3B). This transgene fully rescues the lethality of homozygous

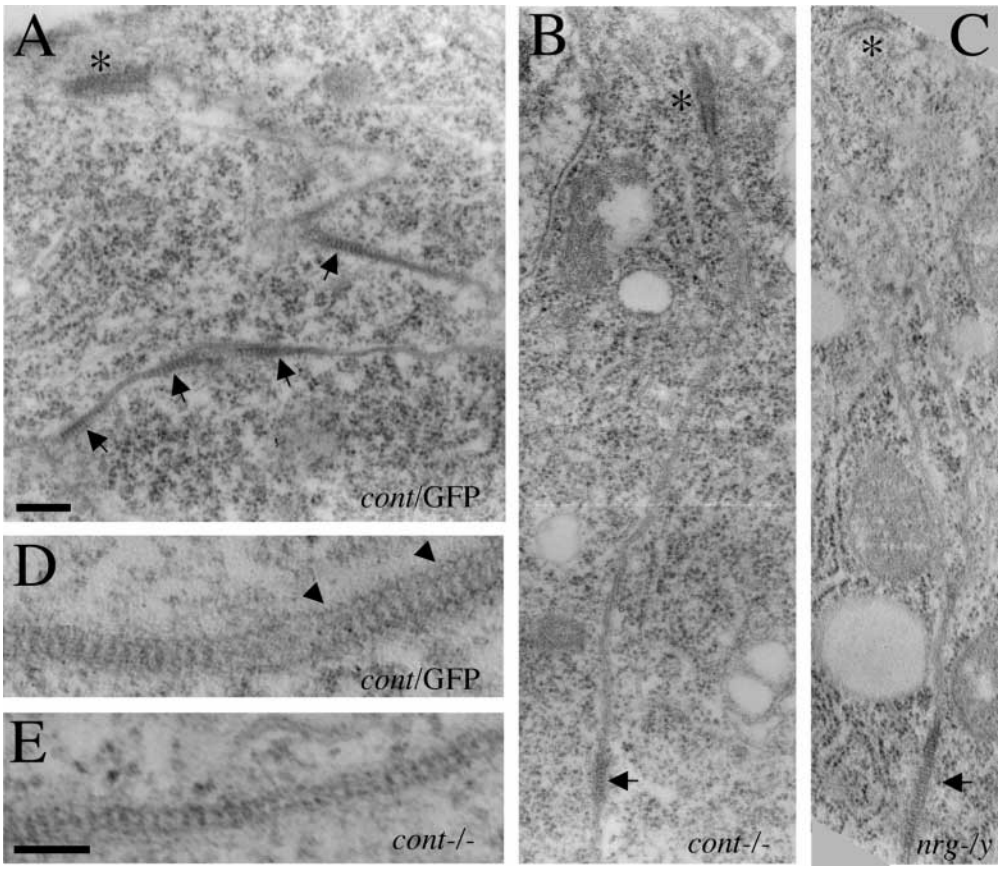

Fig. 5. Organization of SJs is altered in *cont* mutants. Ultrastructural analysis of the epidermal SJs in control heterozygous *cont*/GFP embryos (A,D), homozygous *cont* (B,E) and nrg^{1}/Y mutant embryos (C) at stage 15. Adherens junctions at the apical side are indicated with asterisks. In control *cont*/GFP embryos, SJ strands (arrows) are observed at the level of a convoluted intercellular junction in the apicolateral region (A). Alignments of a small stretch of septa (arrows) are occasionally seen in *cont* (B) and *nrg* (C) mutants, and are often very basal to adherens junctions in these mutant embryos. High-magnification views of SJ strands in control (D) and *cont* mutant (E) embryos show that mutant SJ strands are narrower compared with control SJs. Intramembranous structures display a scalloped appearance in the heterozygous (arrowheads in D) but not in the *cont* mutant, whereas spacing between septa is normal in *cont* mutant. Scale bar: 200 nm for A-C; 100 nm for D,E.

$cont^{ex956}$ excisions. The rescued adults are fully viable, fertile and are indistinguishable from those of the wild-type flies, and have been maintained as a stable stock. Therefore, the lack of CG11739 gene product is not associated with a lethal phenotype. Two additional genes in *Drosophila*, *CG5254* and *CG6782*, which also encode a mitochondrial tricarboxylate-carrier activity, might substitute for *CG11739* function. Our results indicate that the lethality in $cont^{ex956}$ is due to the loss of CONT, and that this excision represents a null allele of *cont*.

Interdependence of CONT, NRX IV and NRG for their SJ localization

Vertebrate NCP1, contactin and NF-155 co-localize at the paranodal SJs (Bhat et al., 2001) and each of these proteins are found to be mislocalized in the mutant backgrounds of one another (Bhat et al., 2001; Boyle et al., 2001). In order to further investigate the analogy between the paranodal and invertebrate SJs, we examined whether CONT, NRX IV and NRG are mutually dependent on each other for their SJ localization. We first analyzed whether the loss of NRX IV would result in the mislocalization of CONT and NRG, and found that *nrx IV*-null mutant embryos exhibit a diffuse distribution of CONT along the basolateral cell membrane as opposed to its sharp localization at the SJs, as seen in the wild-type embryos (compare white arrowheads in Fig. 4B with Fig. 4F). In addition, we observed that CONT immunoreactivity is often associated with intracellular vesicles (Fig. 4F,H, red arrowheads), suggesting that CONT may not be either efficiently transported or stabilized at the cell surface in *nrx IV* mutants. In addition, NRG, which is present at high levels at the SJs in the wild-type embryos (Fig. 4C) is mislocalized in *nrx IV* mutant embryos and shows a more basolateral localization (arrowhead in Fig. 4G). These results indicate that NRX IV is required for proper SJ localization of CONT and NRG.

Similarly, we carried out triple immunostaining of nrg^{1}-null mutants for NRX IV and CONT localization (Fig. 4I-L). In wild-type embryos, NRG is enriched at SJs (see Fig. 4C, green) with a lower level of expression along the basolateral membrane (Fig. 4C, arrowheads). In epithelial cells of *nrg* mutant embryos, the distribution of NRX IV and CONT becomes basolateral (compare arrowheads in Fig. 4J with 4A, and arrowheads in Fig. 4K with 4B) indicating that NRX IV and CONT are dependent on NRG for their SJ localization.

Next, we analyzed *Cont*-null mutant embryos for SJ localization of NRX IV and NRG. As shown in Fig. 4M-P, with the loss of CONT (Fig. 4M), NRX IV and NRG are mislocalized to the basolateral membrane (compare arrowheads in Fig. 4N with 4A, and arrowheads in Fig. 4O with 4C). Taken together, the immunohistochemical analyses of *nrx IV*, *nrg* and *cont*-null mutants demonstrate that these proteins are mutually dependent on each other for their localization to SJs.

CONT expression restores NRX IV and NRG localization to SJs

As shown in the preceding section, the loss of CONT results

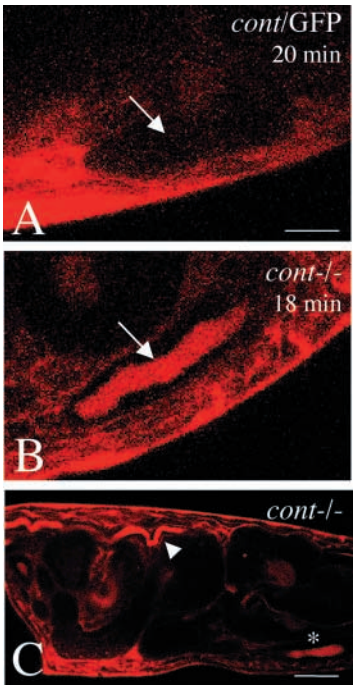

Fig. 6. The paracellular barrier is compromised in *cont* mutant embryos. (A) *cont/GFP* heterozygous late stage embryo injected with rhodamine-labeled dextran into the body cavity reveals an intact paracellular barrier as the dye fails to penetrate into the lumen of the salivary glands 20 minutes after injection (arrow). (B) *cont* mutant embryos injected with the dye into the body cavity reveals breakdown of the paracellular barrier as the dye penetrates into the lumen of the salivary glands within 18 minutes (arrow). (C) *cont* mutant embryos injected with the dye into the body cavity reveals breakdown of the paracellular barrier in the tracheal lumen (arrowhead). The tracheal tube is convoluted in the *cont* mutant embryo. The salivary gland filled with the dye is indicated by an asterisk. Scale bar: 20 μm for A,B; 60 μm for C.

in the mislocalization of NRX IV and NRG to the basolateral membrane. To further demonstrate that the mislocalization phenotype observed in *cont* mutants is due to the loss of CONT only, and not due to any other gene expression disrupted by the P element excision, 4- to 10-hour-old embryos obtained from *hs-cont/hs-cont; cont^{ex956}/TM3,Sb,dfd-lacZ* parental genotype were heat-shocked at 37°C for 60 minutes to induce CONT. After 7 hours incubation at room temperature, the embryos were processed for immunostaining using antibodies against CONT, NRX IV or NRG. *hs-cont/hs-cont; cont^{ex956}/cont^{ex956}* homozygous embryos were identified by the absence of β-galactosidase. As shown in Fig. 4Q-S, induction of CONT expression (4Q, blue) restores the localization of NRX IV to SJs (Fig. 4R, compare arrowheads in 4R with 4A). Similarly, localization of NRG was analyzed in these embryos. As shown in Fig. 4T-V, CONT expression results in the enrichment of NRG at the SJs (compare arrowheads in Fig. 4U with 4C). In addition, the SJ localization of NRX IV and NRG was restored in homozygous *cont^{ex956}* embryos by expression of wild-type CONT from the *Spe*I-*Spe*I genomic rescue fragment (Fig. 4W-Z). Taken together, the rescue experiments demonstrate that CONT is required for the localization of NRX IV and NRG at epithelial SJs, and further strengthen our conclusion that the mislocalization phenotype of NRX IV and NRG is solely due to the loss of CONT in *cont*-null embryos.

CONT is required for SJ organization

To demonstrate the role of CONT in SJ organization, ultrastructural analysis of *cont* mutant embryos was carried out in the epidermis (Fig. 5). In wild-type animals, the pleated SJs are characterized by rows of septa running in the apical half of the lateral membranes, below the adherens junctions. Ultrastructural analysis revealed a complete loss of transverse septa in *nrx IV* mutants (Baumgartner et al., 1996). By contrast, strands of septa are encountered in 92% of *cont* embryos at stage 15 (n=13) (Fig. 5B). However, the wild-type pattern of SJs, which show long stretches of ladder-like structure, was not seen in *cont* mutants and only small clusters of septa were observed occasionally. A quantitative analysis was performed by selecting intercellular junctions that showed strands of septa in the epidermis of *cont* homozygous and *cont*/GFP embryos. As exemplified in Fig. 5A in control *cont*/GFP embryos, septa alignments are mainly found below adherens junctions where the intercellular membranes are very convoluted because of interdigitations of the two opposing cells. These interdigitating membranes with SJs have been previously reported (Noirot-Thimothée and Noirot, 1980). In *cont*/GFP embryos, the mean number of septa in an average SJ is 44.7±1.9 (five embryos, 16 intercellular junctions) whereas in *cont* mutant embryos, intercellular junctions showing such large SJ strands are never found. Whenever any septa are present, they are often more basal in their position (Fig. 5B, arrow), and the mean number of septa is significantly reduced 27.1±3 (six embryos, 23 intercellular junctions scored). At higher magnification, electron dense intramembranous structures on both sides of the junction display a scalloped appearance in *cont*/GFP embryos (Fig. 5D, arrowheads). These intramembranous particles are not distinctly visible in *cont* mutant embryos, suggesting that CONT may be involved in the formation and/or organization of these electron-dense structures (Fig. 5E). Interestingly, the regular spacing between septa (~20-22 nm) does not seem to be affected in *cont* mutants (Fig. 5D,E).

Similarly, we carried out the ultrastructural analysis of *nrg* mutant embryos to determine whether NRG is required for the formation of SJs. Our analysis revealed that occasionally clusters of septa are formed, often basal in their position, in 79% of *nrg^{1}* embryos (n=24) at stage 15 (Fig. 5C). These observations are consistent with the recent study of Genova and Fehon (Genova and Fehon, 2003) that reports a reduced number of septa in *nrg* mutants (see discussion). In conclusion, our results indicate that CONT and NRG are not required for the formation of intermembrane septa, but that they may play a role in organizing the junctional strands of septa in the apicolateral domain to form an effective transepithelial barrier.

CONT is required for epithelial barrier formation

Next, we examined whether CONT plays a role in the transepithelial barrier formation using the method established by Lamb et al. (Lamb et al., 1998). This method relies on the ability of the salivary gland epithelia to exclude rhodamine-dextran (~10 kDa) after its injection into the body cavity of live embryos during late embryogenesis. After the dye injection, confocal sections were acquired on live embryos at time intervals ranging from 10 to 50 minutes. In control

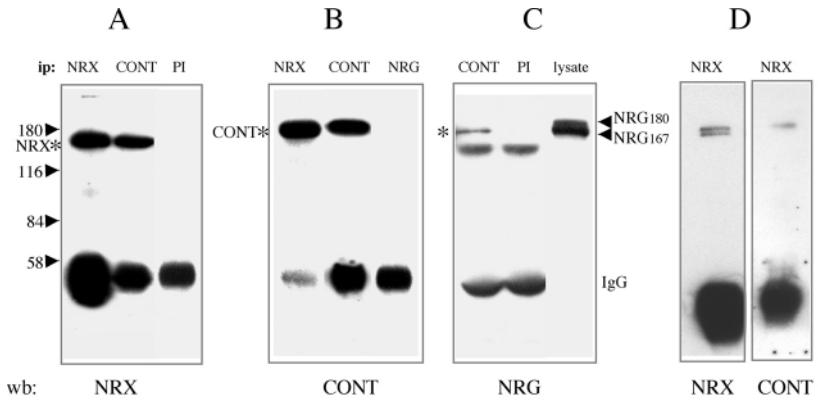

Fig. 7. CONT, NRX IV and NRG form a biochemical complex. Co-immunoprecipitation experiments reveal a tripartite complex between CONT, NRX IV and NRG. NP-40 embryonic lysates were immunoprecipitated with anti-NRX IV, anti-CONT, anti-NRG (1B7) antibodies. Controls were performed with anti-CONT pre-immune serum (PI). Immunoblots were probed with anti-NRX IV (A), rat anti-CONT (B) or anti-NRG 3C1 (C) antibodies. Molecular weight standards in kDa are indicated on the left. NRX IV is co-immunoprecipitated with CONT and reciprocally CONT is co-precipitated with anti-NRX IV antibodies. It was not possible to detect CONT in the anti-NRG immunoprecipitate. By contrast, NRG^{167} (asterisk) was detected in the immunoprecipitate with anti-CONT antibodies. A doublet of both 167 and 180 kDa NRG isoforms is detected in the NP-40 lysate (arrowheads). (D) COS cells were co-transfected with NRX IV and CONT. NP-40 lysate was immunoprecipitated with anti-NRX IV antibody. CONT is detected in the anti-NRX IV immunoprecipitate.

heterozygous *cont*/GFP embryos, the dye remained excluded from the salivary gland lumen after 50 minutes of injection (n=11) (Fig. 6A, arrow). In *cont* mutants, diffusion of the dye into the lumen of salivary glands was observed within 20 minutes of the injection (n=12). Similar kinetics of dye diffusion into salivary gland lumen have been observed for *gliotactin* and *megatrachea* mutants, which display disorganization or absence of septal clusters (Behr et al., 2003; Schulte et al., 2003). None of the *cont* mutants excluded the dye from their lumen (Fig. 6B, arrow). The dye also entered freely in the tracheal lumen of the *cont* mutant embryos (Fig. 6C, arrowhead) in addition to the lumen of the salivary glands (Fig. 6C, asterisk). Thus, the dye exclusion data, in combination with the ultrastructural analysis, demonstrate that CONT is required for the organization and function of the SJs.

CONT, NRX IV and NRG form a biochemical complex

Analyses of *cont*, *nrx IV* and *nrg* mutants showed that these genes display a common alteration of SJ phenotype and thus are required for the formation and/or organization of SJs. In addition, the immunohistochemical analysis of these mutants showed that CONT, NRX IV and NRG are dependent on each other for SJ localization. The phenotypic similarities raised the interesting issue of whether these proteins are part of a macromolecular protein complex that exists at SJs, and thus become dependent on each other for their localization. To determine whether these three proteins form a biochemical complex, microsomal NP-40 extracts were prepared from *Drosophila* embryos and used for co-immunoprecipitation experiments. CONT was efficiently co-immunoprecipitated with NRX IV using either anti-NRX IV or anti-CONT antibodies (Fig. 7A,B). CONT and NRX IV were not co-precipitated by monoclonal anti-NRG antibodies, owing to weak ability to immunoprecipitate NRG complexes. However, by probing western blots with the 3C1 anti-NRG mAb, NRG was detected in anti-CONT immunoprecipitates (Fig. 7C). Only the lower molecular weight NRG^{167} isoform, which is expressed in epithelial cells, was co-immunoprecipitated with CONT. By contrast, the neuronal NRG^{180} isoform could only be detected in the total NP-40 lysate (Fig. 7C, arrowheads). These results demonstrate that CONT, NRX IV and NRG are part of a protein complex and that the molecular interactions between these proteins may underlie the organization of the SJs.

NRX IV is required for the cell surface expression of CONT

The biochemical and immunohistochemical data showed that CONT is part of a protein complex that includes NRX IV and that CONT is mislocalized in *nrx IV* mutants. Furthermore, in these mutants, CONT protein is not expressed properly on the plasma membrane and is seen in intracellular vesicles in the epithelial cells (red arrowheads in Fig. 4F,H). This raised the possibility that NRX IV might be involved in the cell surface targeting or stabilization of CONT. As *Drosophila* S2 cells constitutively express NRX IV and CONT, we addressed this question using neuroblastoma N2a cells as a heterologous expression system. In transfected N2a cells, NRX IV is efficiently expressed at the cell surface (Fig. 8A). By contrast, in cells expressing CONT, the CONT protein appears to remain localized intracellularly and double-staining with the ER marker BiP indicates that CONT is retained in the ER (Fig. 8B-D). Immunofluorescence staining under permeabilizing conditions of N2a cells, which were co-transfected with CONT and NRX IV, revealed that CONT is transported to and co-localized with NRX IV at the plasma membrane (Fig. 8E,F). Similar results were obtained with intact living cells (Fig. 8G,H). Thus, these results indicate that NRX IV mediates the cell-surface targeting of CONT. Next, we co-immunoprecipitated CONT with NRX IV from co-transfected COS cell lysates (Fig. 7D), as a further evidence that these proteins interact in cis. Such a cis-interaction has been reported for their vertebrate counterparts contactin and NCP1 (Peles et al., 1997).

In conclusion, the phenotypic and biochemical studies described here demonstrate that CONT plays a crucial role in SJ formation and function. Furthermore, our results provide evidence that the molecular architecture of SJs has been preserved during evolution making these junctions amenable to further genetic and molecular analysis.

Discussion

In the present study, we show that the contactin gene family plays an evolutionarily conserved function in the organization of SJs. We cloned *Drosophila* contactin and showed that it localizes to SJs and is required for paracellular barrier function. CONT is essential for the localization of NRX IV and NRG at

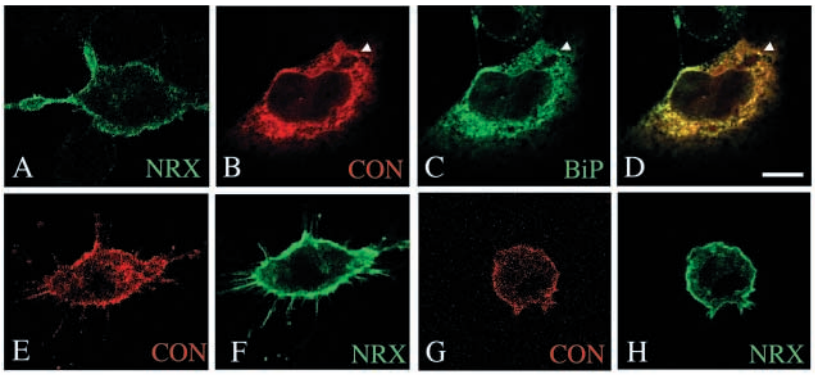

Fig. 8. Cell-surface expression of CONT depends on NRX IV. Neuroblastoma N2a cells were transfected with NRX IV or CONT, or co-transfected with both constructs. (A) NRX IV is efficiently transported to the cell surface in the absence of CONT. (B-D) When transfected alone, CONT is not expressed at the plasma membrane. Double-immunostaining of CONT (B, red) and the ER marker BiP (C, green). The merged image (D) shows that CONT is retained in the ER (arrowheads). (E-H) Co-transfection of CONT (E) and NRX IV (F) in N2a cells results in expression of CONT protein at the plasma membrane. (G,H) Cell-surface expression of CONT in N2a cells co-transfected with CONT and NRX IV. Cells were fixed, permeabilized with Triton X-100 and processed for immunofluorescence staining in A-F. Immunostaining for CONT was carried out on living cells in G and then cells were fixed, permeabilized and processed for NRX IV immunostaining (H). Scale bar: 10 μm.

SJs and these proteins form a tripartite complex. Our studies are inline with the vertebrate studies where homologous cell-adhesion molecules, NCP1 and contactin are required to establish paranodal SJs in complex with NF-155 (Girault and Peles, 2002; Bhat, 2003). In addition, NCP molecules interact with scaffolding proteins of the FERM (4.1, Ezrin, Radixin, Moesin) family, 4.1B and coracle in vertebrate and invertebrate species, respectively (Fehon et al., 1994; Ward et al., 1998; Gollan et al., 2002; Denisenko-Nehrbass et al., 2003). Therefore, the molecular composition of *Drosophila* SJs and vertebrate axo-glial SJs is highly conserved.

Conserved heterophilic binding activities of contactin and NCP molecules

A single representative of the contactin gene family was identified in the *Drosophila* genome, whereas six genes have been identified to date in vertebrates. A phylogenetic analysis indicates that CONT is not a specific ortholog of any one of the vertebrate contactin-type proteins. As CONT is a component of SJs, it appears to be the functional counterpart of vertebrate contactin, which is a component of paranodal SJs. In vertebrates, contactin interacts with NCP1/caspr in cis at the paranodal SJs (Peles et al., 1997), whereas a contactin-related protein TAG-1 has been identified as a glial component of the juxta-paranodes (Traka et al., 2002) and interacts with NCP2/caspr2 (Poliak et al., 1999; Traka et al., 2003). The binding partners for other NCP members are still not known, which may include other members of the contactin family. The *Drosophila* genome encodes only one contactin which interacts with the only member of the *Drosophila* NCP family, NRX IV. Therefore, it seems that heterophilic binding between contactin and NCP molecules has occurred early during evolution and has been conserved following gene duplication in both gene families.

Targeting of the contactin complex to the cell membrane

In vertebrates, efficient transport of NCP1 from the endoplasmic reticulum to the surface of transfected cells requires association with the GPI-linked contactin (Faivre-Sarrailh et al., 2000; Bonnon et al., 2003). NCP1 accumulates intracellularly and fails to be recruited to paranodes in the nerves of contactin-deficient mice demonstrating that contactin is essential for axonal sorting of NCP1 in vivo (Boyle et al., 2001). It came as a surprise, that in *Drosophila*, a different mode of operation appears to control the membrane expression of the contactin-NCP complex and, conversely, NRX IV is required for the distribution of CONT at the cell surface. In *nrx IV* mutant embryos, CONT is not efficiently expressed at the plasma membrane, but rather appears to accumulate in vesicular organelles in the cytoplasm of epithelial cells. In transfected N2a cells, CONT remains associated with the ER and is only efficiently transported to the cell surface upon co-transfection with NRX IV. Such a mechanism of co-targeting would allow the controlled sorting of CONT to the cell surface, where it may essentially be present in a cis-complex with NRX IV.

Role of the CONT, NRX IV, NRG complex in the organization of SJs

CONT, NRX IV and NRG are interdependent for their restricted distribution at the apicolateral membrane, but the molecular arrangement of this ternary complex is still unknown. It has previously been shown that NRX IV does not mediate homophilic adhesion (Baumgartner et al., 1996). As NRX IV is required for transport of CONT to the cell surface, we can assume that the two molecules interact with each other in a cis configuration, within the same plane of the membrane. In the vertebrate paranodal junctions, a ternary complex of NCP1/contactin interacting with NF-155 is crucial for mediating the axo-glial heterotypic contact. A different context is encountered in *Drosophila*, in which SJs occur via the homotypic adhesion of two epithelial or glial cells. NRG is a potent homophilic adhesion molecule (Hortsch et al., 1995). It is currently unknown whether the CONT/NRX IV complex interacts with NRG in a cis- or in a trans-manner.

We and others have shown that NRG is a component of the *Drosophila* SJs in epithelial cells and is involved in the apicolateral restricted distribution of NRX IV and CONT. The ultrastructural analysis reveals that small strands of septa can be formed in the absence of NRG. This is in agreement with the studies of Genova and Fehon (2003), which indicated that mutation in *nrg* disrupts the paracellular barrier in the embryonic salivary gland, and induce alteration of the SJs. Similarly, small strands of septa are occasionally formed in the *cont* mutant, although the organization of these septa in the apical membrane is severely impaired. The transverse septa, which are characteristic of the pleated SJs, are missing in *nrx IV* mutants (Baumgartner et al., 1996) and, therefore, NRX IV is crucial for the assembly of SJ strands. This activity may rely on its interaction with the scaffolding protein coracle, which is also strictly required for septa formation (Lamb et al., 1998).

As NRX IV does not display homophilic binding (Baumgartner et al., 1996), its role in septa formation may also rely on binding with a still unidentified adhesion molecule. Molecular interactions between NRX IV, CONT and NRG are likely to be involved in the organization and lateral positioning of the junctional strands. Therefore, the molecular requirement for septa formation in *Drosophila* is somewhat similar to what has been reported for the vertebrate paranodal SJs. In the mouse, disruption of contactin and NCP1 genes both result in the disappearance of intermembranous septa and disorganization of paranodal junctions (Bhat et al., 2001; Boyle et al., 2001). The loss-of-function analysis of the glial NF-155 should reveal whether NF-155 is required for the formation of paranodal SJs.

Distinct roles for the multiple septate junction molecules

Invertebrate SJs display similar molecular composition and morphology to the vertebrate paranodal junctions, but also display functional analogy with the vertebrate tight junctions by forming a diffusion barrier. A remarkable difference between the septate and tight junctions resides in their ultrastructural morphology. SJs are characterized by rows of intermembrane septa, whereas tight junctions have membrane-kissing points resulting from the sealing of claudin strands (Tepass and Hartenstein, 1994; Morita et al., 1999). Recent studies report the identification of two claudins, megatrachea (Behr et al., 2003) and sinuous (Wu et al., 2004), as components of the *Drosophila* SJs that are essential for the barrier function. This is an indication that the two types of junctions display some molecular similarities in addition to their functional analogy. The question of whether the vertebrate paranodal junctions also contain claudins is still unresolved.

In addition, an increasing number of adhesion proteins have been recently reported to be essential for the organization of invertebrate SJs and formation of the paracellular diffusion barrier, including the Ig-CAM lachesin, and the cholinesterase-like molecule gliotactin (Genova and Fehon, 2003; Schulte et al., 2003; Llimargas et al., 2004). Strikingly, all these components are interdependent for their distribution at SJs [e.g. NRX IV is mislocalized to the basolateral membrane in *megatrachea*, *sinuous*, *gliotactin*, or *lachesin* mutant embryos (Behr et al., 2003; Schulte et al., 2003; Llimargas et al., 2004; Wu et al., 2004)]. A lack of intermembrane septa has been observed in *lachesin* (Llimargas et al., 2004) and *megatrachea* (Behr et al., 2003) mutants, whereas *sinuous* mutant embryos display a phenotype similar to the *cont* mutant, showing some strands of septa that are disorganized (Wu et al., 2004). A unique function has been proposed for gliotactin that only colocalizes with other SJ markers at the tricellular junctions. Ultrastructural analysis indicated that septa are present in the *gliotactin* mutant but the rows of septa are not tightly arrayed, and gliotactin may serve as an anchor at the tricellular corners and induce apical compaction of the SJ strands (Schulte et al., 2003). Now, the question that arises is what is molecular interplay between all these SJ markers? The future challenges would be to molecularly dissect the structural elements forming the intermembrane septa, and finding out how the distinct SJ components determine elongation of the strands and compaction of the parallel rows in the apical half of epithelial cell membrane, that is central to establishing an effective diffusion barrier.

This work was supported by the Association pour la Recherche sur la Sclérose en Plaques, the Mizutani Foundation for Glycosciences, the Fondation pour la Recherche Médicale (C.F.-S.), Howard Temin Career Development Award from the National Cancer Institute, KO1-CA 78437 (M.A.B.), Hirschl Foundation Career Development Award (M.A.B.), NIH grants GM63074 (M.A.B.) and HD 29388 (M.H.), and NSF grant IBN-0132819 (M.H.). We thank Afshan Ismat for *Spe*I genomic construct, and André Le Bivic, Michel Piovant, Luis Garcia-Alonso and members of the Bhat laboratory for helpful discussions.

References

Auld, V. J., Fetter, R. D., Broadie, K. and Goodman, C. S. (1995). Gliotactin, a novel transmembrane protein on peripheral glia, is required to form the blood-nerve barrier in *Drosophila*. *Cell* **81**, 757-767.

Baumgartner, S., Littleton, J. T., Broadie, K., Bhat, M. A., Harcke, R., Lengyel, J. A., Chiquet Ehrismann, R., Prokop, A. and Bellen, H. J. (1996). A *Drosophila* neurexin is required for septate junction and blood-nerve barrier formation and function. *Cell* **13**, 1059-1068.

Behr, M., Riedel, D. and Schuh, R. (2003). The claudin-like megatrachea is essential in septate junctions for the epithelial barrier function in *Drosophila*. *Dev. Cell* **5**, 611-620.

Bellen, H. J., Lu, Y., Beckstead, R. and Bhat, M. A. (1998). Neurexin IV, Caspr and paranodin-novel members of the neurexin family, encounters of axons and glia. *Trends Neurosci.* **10**, 444-449.

Berglund, E. O., Murai, K., Fredette, B., Sekerkova, G., Marturano, B., Weber, L., Mugnaini, E. and Ranscht, B. (1999). Ataxia and abnormal cerebellar microorganization in mice with ablated contactin gene expression. *Neuron* **24**, 739-750.

Bhat, M. A. (2003). Molecular organization of axo-glial junctions. *Curr. Opin. Neurobiol.* **13**, 552-559.

Bhat, M. A., Izaddoost, S., Lu, Y., Cho, K. O., Choi, K. W. and Bellen, H. J. (1999). Discs Lost, a novel multi-PDZ domain protein, establishes and maintains epithelial polarity. *Cell* **96**, 833-845.

Bhat, M. A., Rios, J. C., Lu, Y., Garcia-Fresco, G. P., Ching, W., Martin, M. S., Li, J., Einheber, S., Chesler, M., Rosenbluth, J. et al. (2001). Axon-glia interactions and the domain organization of myelinated axons require neurexin IV/caspr/paranodin. *Neuron* **30**, 369-383.

Bieber, A. J., Snow, P. M., Hortsch, M., Patel, N. H., Jacobs, J. R., Traquina, Z. R., Schilling, J. and Goodman, C. S. (1989). *Drosophila* neuroglian, a member of the immunoglobulin superfamily with extensive homology to the vertebrate neural adhesion molecule L1. *Cell* **59**, 447-460.

Bonnon, C., Goutebroze, L., Denisenko-Nehrbass, N., Girault, J. A. and Faivre-Sarrailh, C. (2003). The paranodal complex of F3/contactin and caspr/paranodin traffics to the cell surface via a non-conventional pathway. *J. Biol. Chem.* **278**, 48339-48347.

Boyle, M. E., Berglund, E. O., Murai, K. K., Weber, L., Peles, E. and Ranscht, B. (2001). Contactin orchestrates assembly of the septate-like junctions at the paranode in myelinated peripheral nerve. *Neuron* **30**, 385-397.

Brümmendorf, T. and Rathjen, F. (1996). Structure/function relationships of axon-associated adhesion receptors of the immunoglobulin superfamily. *Curr. Opin. Neurobiol.* **6**, 584-592.

Charles, P., Tait, S., Faivre-Sarrailh, C., Barbin, G., Gunn-Moore, F., Denisenko-Nehrbass, N., Guennoc, A. M., Girault, J. A., Brophy, P. J. and Lubetzki, C. (2002). Neurofascin is a glial receptor for the paranodin/Caspr-contactin axonal complex at the axoglial junction. *Curr. Biol.* **12**, 217-220.

Denisenko-Nehrbass, N., Oguievetskaia, K., Goutebroze, L., Galvez, T., Yamakawa, H., Ohara, O., Carnaud, M. and Girault, J. A. (2003). Protein 4.1B associates with both Caspr/paranodin and Caspr2 at paranodes and juxtaparanodes of myelinated fibres. *Eur. J. Neurosci.* **17**, 411-416.

Einheber, S. and Salzer, J. L. (2000). A glial investment of axons defrayed. *Neuron* **28**, 627-628.

Faivre-Sarrailh, C., Gauthier, F., Denisenko-Nehrbass, N., le Bivic, A., Rougon, G. and Girault, J. A. (2000). The GPI-anchored adhesion molecule F3/contactin is required for surface transport of paranodin/caspr. *J. Cell Biol.* **149**, 491-502.

Falk, J., Bonnon, C., Girault, J. A. and Faivre-Sarrailh, C. (2002). F3/contactin, a neuronal cell adhesion molecule implicated in axogenesis and myelination. *Biol. Cell.* **94**, 327-334.

Fehon, R. G., Dawson, I. A. and Artavanis-Tsakonas, S. (1994). A *Drosophila* homologue of membrane-skeleton protein 4.1 is associated with

septate junctions and is encoded by the coracle gene. *Development* **120**, 545-557.

Furley, A. J., Morton, S. B., Manalo, D., Karagogeos, D., Dodd, J. and Jessell, T. M. (1990). The axonal glycoprotein TAG-1 is an immunoglobulin superfamily member with neurite outgrowth promoting activity. *Cell* **61**, 157-170.

Gennarini, G., Cibelli, G., Rougon, G., Mattei, M. and Goridis, C. (1989). The mouse neuronal cell surface protein F3, a phosphatidylinositol-anchored member of the immunoglobulin superfamily related to the chicken contactin. *J. Cell Biol.* **109**, 775-788.

Genova, J. L. and Fehon, R. G. (2003). Neuroglian, gliotactin, and the Na+/K+ ATPase are essential for septate junction function in *Drosophila*. *J. Cell Biol.* **161**, 979-989.

Girault, J. A. and Peles, E. (2002). Development of nodes of Ranvier. *Curr. Opin. Neurobiol.* **12**, 476-485.

Gollan, L., Sabanay, H., Poliak, S., Berglund, E. O., Ranscht, B. and Peles, E. (2002). Retention of a cell adhesion complex at the paranodal junction requires the cytoplasmic region of Caspr. *J. Cell Biol.* **157**, 1247-1256.

Hortsch, M. (2000). Structural and functional evolution of the L1 family, are four adhesion molecules better than one? *Mol. Cell. Neurosci.* **15**, 1-10.

Hortsch, M. and Goodman, C. S. (1990). *Drosophila* Fasciclin I, a neural cell adhesion molecule, has a phosphatidylinositol lipid memebrane anchor that is developmentally regulated. *J. Biol. Chem.* **265**, 15104-15109.

Hortsch, M., Wang, Y. M., Marikar, Y. and Bieber, A. J. (1995). The cytoplasmic domain of the *Drosophila* cell adhesion molecule neuroglian is not essential for its homophilic adhesive properties in S2 cells. *J. Biol. Chem.* **270**, 18809-18817.

Kirkpatrick, C. and Peifer, M. (1995). Not just glue, cell-cell junctions as cellular signaling centers. *Curr. Opin. Genet. Dev.* **5**, 56-65.

Lamb, R. S., Ward, R. E., Schweizer, L. and Fehon, R. G. (1998). *Drosophila coracle*, a member of the protein 4.1 superfamily, has essential structural functions in septate junctions and developmental functions in embryonic and adult epithelial cells. *Mol. Biol. Cell* **9**, 3505-3519.

Llimargas, M., Strigini, M., Katidou, M., Karagogeos, D. and Casanova, J. (2004). Lachesin is a component of a septate junction-based mechanism that controls tube size and epithelial integrity in the *Drosophila* tracheal system. *Development*, **131**, 181-190.

Menegoz, M., Gaspar, P., le Bert, M., Galvez, T., Burgaya, F., Palfrey, C., Ezan, P., Arnos, F. and Girault, J. A. (1997). Paranodin, a glycoprotein of neuronal paranodal membranes. *Neuron* **19**, 319-331.

Morita, K., Furuse, M., Fujimoto, K. and Tsukita, S. (1999). Claudin multigene family encoding four-transmembrane domain protein components of tight junction strands. *Proc. Natl. Acad. Sci. USA* **96**, 511-516.

Noirot-Thimothé, C. and Noirot, C. (1980). Septate and scalariform junctions in arthropods. *Int. J. Cytol.* **63**, 97-140.

Ogawa, J., Kaneko, H., Masuda, T., Nagata, S., Hosoya, H. and Wattman, K. (1996). Novel neural adhesion molecules in the Contactin/F3 subgroup of the immunoglobulin superfamily, isolation and characterization of cDNAs from rat brain. *Neurosci. Lett.* **218**, 173-176.

Peles, E., Nativ, M., Lustig, M., Grumet, M., Schilling, J., Martinez, R., Plowman, G. D. and Schlessinger, J. (1997). Identification of a novel contactin-associated transmembrane receptor with multiple domains implicated in protein-protein interactions. *EMBO J.* **16**, 978-988.

Plagge, A., Sendtner-Voelderndorff, L., Sirim, P., Freigang, J., Rader, C., Sonderegger, P. and Brümmendorf, T. (2001). The contactin-related protein FAR-2 defines Purkinje cell clusters and labels subpopulations of climbing fibers in the developing cerebellum. *Mol. Cell. Neurosci.* **18**, 91-107.

Poliak, S., Gollan, L., Martinez, R., Custer, A., Einheber, S., Salzer, J. L., Trimmer, J. S., Shrager, P. and Peles, E. (1999). Caspr2, a new member of the neurexin superfamily, is localized at the juxtaparanodes of myelinated axons and associates with K^+ channels. *Neuron* **24**, 1037-1047.

Rios, J. C., Rubin, M., St Martin, M., Downey, R. T., Einheber, S., Rosenbluth, J., Levinson, S. R., Bhat, M. A. and Salzer, J. L. (2003). Paranodal interactions regulate expression of sodium channel subtypes and provide a diffusion barrier for the node of Ranvier. *J. Neurosci.* **23**, 7001-7011.

Schulte, J., Tepass, U. and Auld, V. J. (2003). Gliotactin, a novel marker of tricellular junctions, is necessary for septate junction development in *Drosophila*. *J. Cell Biol.* **161**, 991-1000.

Tamkun, J. W., Deuring, R., Scott, M. P., Kissinger, M., Pattatucci, A. M., Kaufmann, T. C. and Kennison, J. A. (1992). *brahma*, a regulator of *Drosophila* homeotic genes structurally related to the yeast transcriptional activator SNF2/SWI2. *Cell* **68**, 561-572.

Tepass, U. and Hartenstein, V. (1994). The development of cellular junctions in the *Drosophila* embryo. *Dev. Biol.* **161**, 563-596.

Thummel, C. S., Boulet, A. M. and Lipshitz, H. D. (1988). Vectors for *Drosophila* P-element-mediated transformation and tissue culture transfection. *Gene* **74**, 445-456.

Traka, M., Dupree, J. L., Popko, B. and Karagogeos, D. (2002). The neuronal adhesion protein TAG-1 is expressed by Schwann cells and oligodendrocytes and is localized to the juxtaparanodal region of myelinated fibers. *J. Neurosci.* **22**, 3016-3024.

Traka, M., Goutebroze, L., Denisenko, N., Bessa, M., Nifli, A., Havaki, S., Iwakura, Y., Fukamauchi, F., Watanabe, K., Soliven, B. et al. (2003). Association of TAG-1 with Caspr2 is essential for the molecular organization of juxtaparanodal regions of myelinated fibers. *J. Cell Biol.* **162**, 1161-1172.

Ward, R. E., Lamb, R. S. and Fehon, R. G. (1998). A conserved functional domain of *Drosophila coracle* is required for localization at the septate junction and has membrane-organizing activity. *J. Cell Biol.* **140**, 1463-1473.

Willott, E., Balda, M. S., Fanning, A. S., Jameson, B., van Itallie, C. and Anderson, J. M. (1993). The tight junction protein ZO-1 is homologous to the *Drosophila* discs-large tumor suppressor protein of septate junctions. *Proc. Natl. Acad. Sci. USA* **90**, 7834-7838.

Woods, D. F., Hough, C., Peel, D., Callaini, G. and Bryant, P. J. (1996). Dlg protein is required for junction structure, cell polarity, and proliferation control in *Drosophila* epithelia. *J. Cell Biol.* **134**, 1469-1482.

Wu, V. M., Schulte, J., Hirschi, A., Tepass, U. and Beitel, G. J. (2004). Sinuous is a *Drosophila* claudin required for septate junction organization and epithelial tube size control. *J. Cell Biol.* **164**, 313-323.

Yoshihara, Y., Kawasaki, M., Tamada, A., Nagata, S., Kagamiyama, H. and Mori, K. (1995). Overlapping and differential expression of BIG-2, BIG-1, TAG-1, and F3, four members of an axon-associated cell adhesion molecule subgroup of the immunoglobulin superfamily. *J. Neurobiol.* **28**, 51-69.